The *Justy* mutation identifies *Gon4-like* as a gene that is essential for B lymphopoiesis

Ping Lu,[4] Isaiah L. Hankel,[2] Judit Knisz,[1] Andreas Marquardt,[5] Ming-Yi Chiang,[4] Johannes Grosse,[5] Rainer Constien,[5] Thomas Meyer,[5] Andreas Schroeder,[5] Lutz Zeitlmann,[5] Umaima Al-Alem,[6] Ann D. Friedman,[1] Eric I. Elliott,[1] David K. Meyerholz,[3] Thomas J. Waldschmidt,[3,4] Paul B. Rothman,[1,4] and John D. Colgan[1,2,4]

[1]Department of Internal Medicine, [2]Department of Anatomy and Cell Biology, [3]Department of Pathology, and [4] the Immunology Graduate Program, Roy J. and Lucille A. Carver College of Medicine, University of Iowa, Iowa City, IA 52242
[5]Ingenium Pharmaceuticals, 82152 Martinsried, Germany
[6]Columbia University College of Physicians and Surgeons, New York, NY 10032

A recessive mutation named *Justy* was found that abolishes B lymphopoiesis but does not impair other major aspects of hematopoiesis. Transplantation experiments showed that homozygosity for *Justy* prevented hematopoietic progenitors from generating B cells but did not affect the ability of bone marrow stroma to support B lymphopoiesis. In bone marrow from mutant mice, common lymphoid progenitors and pre-pro–B cells appeared normal, but cells at subsequent stages of B lymphopoiesis were dramatically reduced in number. Under culture conditions that promoted B lymphopoiesis, mutant pre-pro–B cells remained alive and began expressing the B cell marker CD19 but failed to proliferate. In contrast, these cells were able to generate myeloid or T/NK precursors. Genetic and molecular analysis demonstrated that *Justy* is a point mutation within the *Gon4-like* (*Gon4l*) gene, which encodes a protein with homology to transcriptional regulators. This mutation was found to disrupt Gon4l pre-mRNA splicing and dramatically reduce expression of wild-type Gon4l RNA and protein. Consistent with a role for Gon4l in transcriptional regulation, the levels of RNA encoding C/EBPα and PU.1 were abnormally high in mutant B cell progenitors. Our findings indicate that the Gon4l protein is required for B lymphopoiesis and may function to regulate gene expression during this process.

CORRESPONDENCE
John Colgan:
john-colgan@uiowa.edu

Abbreviations used: CLP, common lymphoid progenitor; Gon4l, Gon4-like; PAH, paired amphipathic helix; pDC, plasmacytoid DC; SSLP, simple sequence length polymorphism.

Hematopoietic progenitor cells progress through pathways that restrict developmental plasticity and enforce commitment to specific lineages (Laiosa et al., 2006; Brown et al., 2007). These processes coincide with gene expression remodeling as orchestrated by a transcription factor network (Laiosa et al., 2006; Nutt and Kee, 2007). Many DNA-binding components of this network are known, but how these proteins coordinately regulate gene expression is poorly understood. Also, disruption of the hematopoietic transcription factor network is strongly associated with oncogenesis (O'Neil and Look, 2007; Rosenbauer and Tenen, 2007). Thus, further characterizing the mechanisms that control hematopoiesis could provide insights regarding neoplasia in this system.

Among hematopoietic developmental pathways, B lymphopoiesis is well defined (Hardy et al., 2007; Welner et al., 2008). During this process, the transcription factors Ikaros, E2A, EBF, and Pax5 likely function to recruit protein complexes that activate B-lineage genes or repress genes associated with other lineages (Ng et al., 2007; Nutt and Kee, 2007). Consistent with this idea, gene activation by EBF and Pax5 involves the chromatin-remodeling complex SWI–SNF, whereas Ikaros or Pax5 can interact with transcriptional corepressors (Eberhard et al., 2000; Koipally and Georgopoulos, 2002; Gao et al., 2009). Interactions between B cell transcription factors and unknown cofactors are

P. Lu, I.L. Hankel, and J. Knisz contributed equally to this paper.

The Rockefeller University Press $30.00
J. Exp. Med. Vol. 207 No. 7 1359-1367
www.jem.org/cgi/doi/10.1084/jem.20100147

The Journal of Experimental Medicine

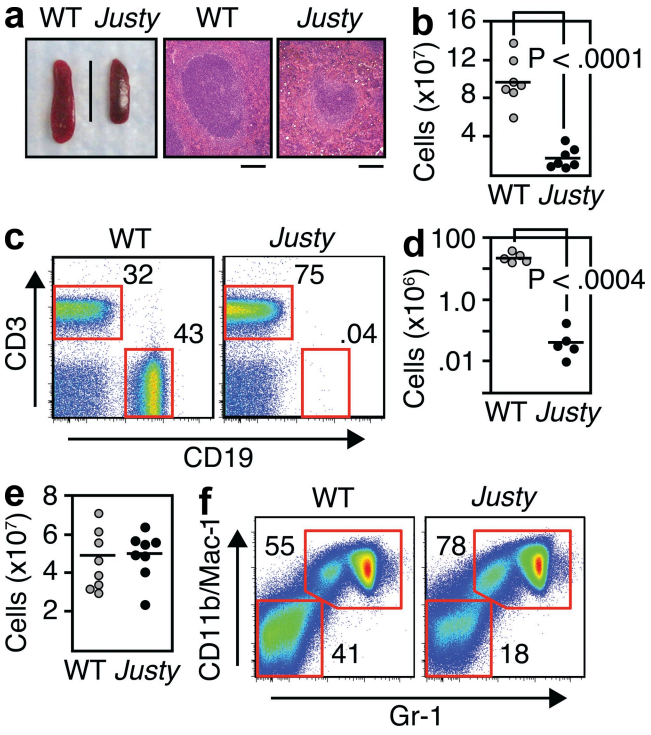

Figure 1. *Justy* mice lack B cells. (a) Spleens and hematoxylin/eosin-stained spleen sections (100× magnification). Bars: (left) 1 cm; (right) 225 µm. (b) Cell yields from wild-type and *Justy* spleens. (c) Flow cytometric analysis of splenocytes. (d) CD19+ cell yields from splenocyte preparations. (e) Leukocyte yields from bone marrow cell preparations. (f) Flow cytometric analysis of bone marrow cells. Horizontal bars in b, d, and e indicate mean cell count. Data in c and f are representative of five independent experiments.

also likely important for immunoglobulin gene rearrangement (Fuxa et al., 2004; Reynaud et al., 2008). Thus, although much has been defined, significant gaps remain in our knowledge of how gene expression is regulated during B lymphopoiesis.

Mice bearing random mutations are powerful tools for identifying genes with roles in the immune system (Cook et al., 2006; Beutler et al., 2007). In this paper, we describe a chemically induced recessive mutation that blocks B lymphopoiesis at an early stage without perturbing the development of other hematopoietic lineages. This lesion is a point mutation that reduces RNA and protein expression from *Gon4-like* (*Gon4l*), which likely encodes a novel regulator of gene expression. The mutation had little impact on B-lineage gene expression but impaired the regulation of genes associated with myeloid cell development. Our findings demonstrate that *Gon4l* is critical for B lymphopoiesis.

RESULTS AND DISCUSSION

Justy mice lack peripheral B cells

Male C3HeB/FeJ (C3H) mice were injected with a dose of *n*-ethyl-*n*-nitrosourea that resulted in ~1 mutation per 2.7 megabase pairs of DNA (Hrabé de Angelis et al., 2000; Augustin et al., 2005) and were mated to wild-type C3H females. F1 males were screened by flow cytometry to identify mice with normal peripheral blood that might be carriers of recessive mutations. These mice were mated to wild-type C3H females and then to the resulting F2 females. Flow cytometric analysis identified F3 mice that lacked blood cells expressing the B-lineage marker CD45R/B220 (B220). These mice were crossed to wild-type C3H mice, and the progeny were used for brother–sister matings. Offspring lacking B220+ cells were crossed to wild-type C3H mice, and the progeny were used for brother–sister matings to recover mice that were homozygous for the causal mutation. These mice are fertile and have a normal life span but lack serum immunoglobulin and fail to generate antibodies when challenged with antigens (unpublished data). The mutant strain was named *Justy* (just T cells). In the text that follows, mice homozygous for the mutation are called *Justy* mice.

Spleens from *Justy* mice were abnormally small, had hypoplastic white pulp, and yielded significantly fewer cells than wild-type organs (Fig. 1, a and b). Flow cytometric analysis showed that the frequency and number of CD19+ cells in *Justy* spleens were dramatically decreased (Fig. 1, c and d) and that lymph nodes or peritoneal lavages from *Justy* mice lacked CD19+ cells (not depicted). T and NK cell populations were characterized by flow cytometry (unpublished data). The number of CD3+ cells in *Justy* spleens was consistently decreased by approximately twofold, but otherwise no abnormalities affecting T cells were found. Likewise, NK cells in thymus and spleen appeared normal in *Justy* mice. The cellularity of

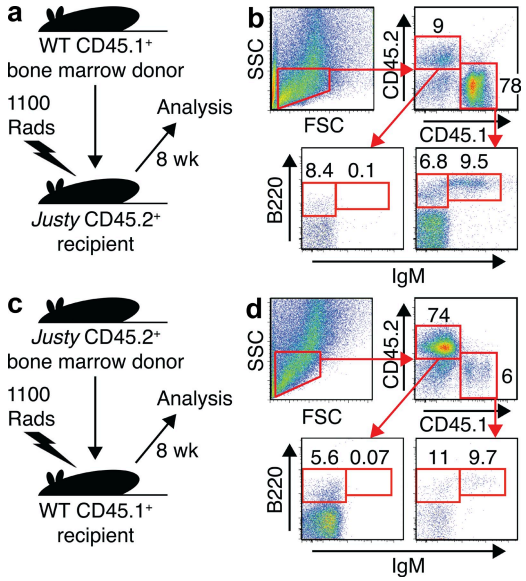

Figure 2. The *Justy* mutation intrinsically affects hematopoietic progenitors. (a and c) Diagrams of bone marrow transplants performed. (b) Flow cytometric analysis of bone marrow from a *Justy* mouse that received CD45.1+ wild-type bone marrow. (d) Flow cytometric analysis of bone marrow from a wild-type mouse that received CD45.2+ *Justy* bone marrow. Data in b and d are representative of two independent transplantation experiments, each involving three recipients that received pooled bone marrow from two donors.

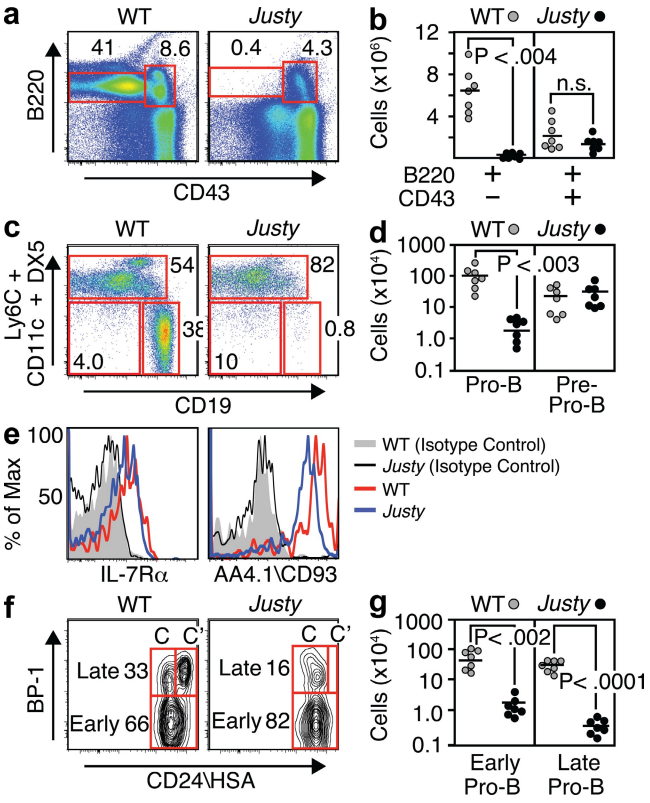

Figure 3. B lymphopoiesis in *Justy* mice arrests at the early pro–B cell stage. (a) Flow cytometric analysis of bone marrow. The $B220^+CD43^-$ gate contains pre–B and immature B cells; the $B220^+CD43^+$ gate contains pre-pro–B and pro–B cells, NK cell precursors, and pDCs. (b) Yields of $B220^+CD43^-$ and $B220^+CD43^+$ cells from bone marrow. (c) Flow cytometric analysis of $B220^+CD43^+$ cells (right gate in a). Pro–B cells are in the $CD19^+Ly6C^-CD11c^-CD49b^-$ gate; pre-pro–B cells are in the quadruple-negative gate. (d) Yields of pro–B and pre-pro–B cells from bone marrow. (e) Flow cytometric analysis of pre-pro–B cells (from gate in c). (f) Flow cytometric analysis of pro–B cells (from gate in c). (g) Yields of early and late pro–B cells from bone marrow. Data in a, c, e, and f are representative of five independent experiments. Horizontal bars in b, d, and g indicate mean cell count.

Justy bone marrow was similar to that of wild type (Fig. 1 e), but the ratio between myeloid and lymphoid cells was increased (Fig. 1 f), indicating that the mutation affects this anatomical site.

The effect of the *Justy* mutation is intrinsic to hematopoietic progenitors

Reciprocal bone marrow transplants were performed to assess how the mutation affects hematopoietic progenitors and bone marrow stroma. Wild-type bone marrow restored hematopoiesis when transplanted into *Justy* mice and donor-derived $B220^+IgM^+$ cells were detected in bone marrow (and spleen), indicating that *Justy* stroma can support B lymphopoiesis (Fig. 2, a and b). The few host-derived cells present lacked $B220^+IgM^+$ cells, suggesting that introduction of wild-type cells failed to induce B lymphopoiesis from *Justy* cells. *Justy* bone marrow rescued hematopoiesis when transplanted into wild-type mice but donor-derived $B220^+IgM^+$ cells were not detected, indicating that wild-type stroma could not rescue B lymphopoiesis from *Justy* cells (Fig. 2, c and d). $B220^+IgM^+$ cells were detected in host-derived bone marrow, suggesting that *Justy* cells did not suppress B lymphopoiesis from wild type. Thus, the *Justy* mutation has an intrinsic effect on hematopoietic progenitors.

The *Justy* mutation blocks the generation of pro–B cells

Flow cytometric analysis was performed to define how *Justy* affects bone marrow. Because the $Mac\text{-}1^+Gr\text{-}1^+$ compartment in *Justy* bone marrow is enlarged (Fig. 1 f; Fig. S1 a), myeloid progenitors were characterized. The frequency and total number of cells defined as myeloid/granulocytic/erythroid progenitors ($Lin^-IL\text{-}7R\alpha^-Sca\text{-}1^-c\text{-}Kit^+$ cells; Akashi et al., 2000) were consistently but modestly increased in *Justy* bone marrow relative to wild type (Fig. S1, b and c). Based on CD34 and FcγR expression, these differences were a result of proportionate increases in the number of all progenitors in the fraction (unpublished data). These alterations could reflect cell-intrinsic effects or may arise as a result of the void created from the absence of B cells (see following paragraph). The frequency and number of LSK ($Lin^-IL\text{-}7Ra^-Sca\text{-}1^+c\text{-}Kit^+$) cells in *Justy* bone marrow were normal (Fig. S1, b and d), suggesting that the multipotent stem cell pool is not grossly perturbed.

B cell progenitors were also examined. $B220^+CD43^-$ cells comprising B and immature B cells were decreased ∼300-fold in *Justy* bone marrow relative to wild type (Fig. 3, a and b). However, the frequency and number of $B220^+CD43^+$ cells in *Justy* bone marrow were close to normal (Fig. 3, a and b). This population contains cells defined as pro–B and pre-pro–B cells but also includes NK cell precursors and plasmacytoid DCs (pDCs). To distinguish these subsets, expression of CD19, the NK marker CD49b (clone DX5), and the pDC markers CD11c and Ly6C by $B220^+CD43^+$ cells was assessed (Fig. 3 c). Relative to wild type, the frequency and number of pro–B cells ($CD49b^-CD11c^-Ly6C^-CD19^+$) in *Justy* bone marrow were greatly decreased, but these parameters were normal for pre-pro–B cells (quadruple-negative cells; Fig. 3, c and d). Surface levels of IL-7 receptor α and AA4.1/CD93 on *Justy* pre-pro–B cells were similar to that on wild type (Fig. 3 e). Common lymphoid progenitors (CLPs) are a primary source of B cell progenitors. Therefore, these cells were also characterized (Fig. S2 a). Markers examined included Ly6d, which identifies CLPs with potent B cell potential (Inlay et al., 2009; Mansson et al., 2010). These studies demonstrated that the phenotype and number (Fig. S2 b) of CLPs in *Justy* bone marrow were normal.

Differential expression of BP-1 subdivides the pro–B cell compartment into late pro–B cells ($HSA^{hi}BP\text{-}1^+$) and early pro–B cells ($HSA^{hi}BP\text{-}1^-$), whereas differential expression of CD24/HSA subdivides late pro–B cells into fractions C and C′,

with the latter containing cells expressing pre–B cell receptors. Fraction C′ cells were absent from *Justy* bone marrow, but fraction C and early pro–B cells were detectable (Fig. 3 f). However, relative to wild type, the numbers of these cells were dramatically decreased (Fig. 3 g). These data demonstrate that B lymphopoiesis in *Justy* mice is disrupted starting at the early pro–B cell stage.

Justy B cell progenitors specifically lack B cell potential

Pre-pro–B cells, as defined in the previous section, can give rise to early pro–B cells in culture (Rumfelt et al., 2006). To assess how the mutation affects the developmental potential of pre-pro–B cells, these cells were sort purified from wild-type or *Justy* bone marrow and added to stromal cell monolayers under conditions that promote B lymphopoiesis. 10 d later, surface marker phenotypes and cell yields were assessed by flow cytometry (Fig. 4, a and c). Wild-type pre-pro–B cells proliferated extensively and gave rise to $B220^+CD19^+$ cells. In contrast, although *Justy* cells could generate $B220^+CD19^+$ cells, the yield was much lower compared with that from wild type. The responses of sort-purified early pro–B cells to these conditions were also assessed (Fig. 4, b and c). Wild-type cells underwent robust proliferation, as expected, whereas *Justy* cells remained alive, as judged by vital dye exclusion, but failed to expand. IL-7/Stat5 signaling drives B cell proliferation in the culture system. When analyzed immediately after removal from mice, similar levels of surface IL-7 receptor α and intracellular tyrosine-phosphorylated Stat5 were detected in wild-type and *Justy* B cell progenitors (Fig. 3 e; Fig. S3), suggesting that the mutation does not impair receptor-proximal IL-7 signaling. These data indicate that the *Justy* mutation impairs the development of early pro–B cells from progenitors. Alternatively (or in addition), the mutation may prevent early pro–B cells that develop from responding to the appropriate stimuli.

Pre-pro–B cells can generate cells expressing myeloid or T/NK markers (Balciunaite et al., 2005; Rumfelt et al., 2006). Under conditions that favor B lymphopoiesis but permit myeloid cell development, wild-type and *Justy* pre-pro–B cells both generated cells expressing the macrophage/pDC marker Ly6C (Fig. 4, d and f). Likewise, wild-type and *Justy* pre-pro–B cells both produced $B220^-Thy1.2^+CD49b^+$ cells under conditions that promote T/NK cell precursor development (Fig. 4, e and f). Thus, *Justy* pre-pro–B cells retain the capacity to differentiate toward these alternative lineages.

The *Justy* mutation disrupts splicing of RNA transcribed from the *Gon4l* gene

To identify the genetic basis for the phenotype, C3H *Justy* mice were crossed to wild-type B6 mice and F1 progeny were interbred. Genomic DNA from F2 mice that lacked or contained B cells was screened with a panel of PCR primers that detect simple sequence length polymorphisms (SSLPs) between C3H and B6 and thus define the strain of origin for discrete genomic intervals. This analysis established a complete association between a lack of B cells and a 617-kb-pair region on chromosome 3 from C3H between SSLPs D3Mit49 and D3Mit175 (bps 88353984 and 88971024; University of California, Santa Cruz (UCSC) assembly, July 2007). The SSLPs were used to transfer the C3H segment into the B6 background via serial backcrossing. Intercrossing F10 B6 mice generated offspring that were homozygous for the C3H region with Mendelian frequency. Flow cytometric analysis showed that B lymphopoiesis in these mice is blocked, as seen in the original mutant strain (unpublished data), confirming that the transferred C3H DNA segment contained the causative lesion.

The identified region encodes 13 genes (Fig. 5 a and Table S1). Quantitative (Q) RT-PCR analysis of RNA from bone marrow lineage-negative cells showed that all of these genes were expressed normally in *Justy* cells except for *Gon4l*, which was expressed at approximately twofold lower levels relative to wild type (Fig. 5 b). RT-PCR analysis was performed to define the structure of Gon4l mRNA expressed in wild-type and *Justy* cells, which revealed a striking difference (Fig. 5 c). Primers targeting exons 24 and 26 amplified a 446-bp product from wild-type cDNA with the expected sequence. The same product was amplified from *Justy* cDNA

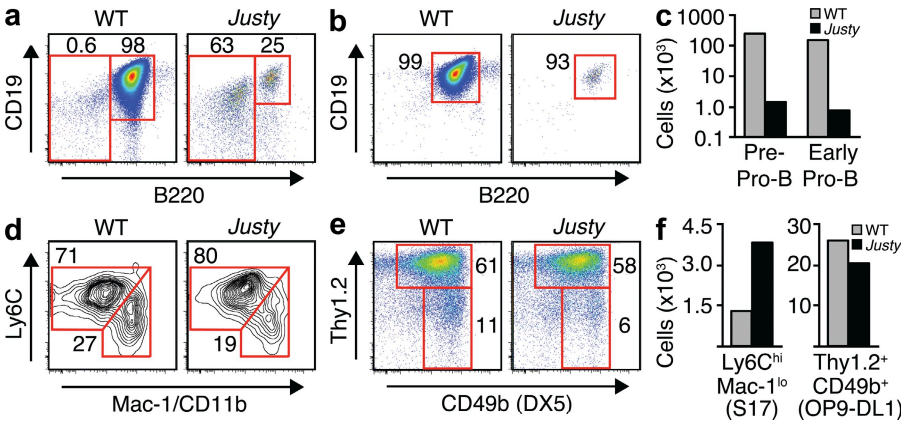

Figure 4. *Justy* B cell progenitors lack B cell potential but retain myeloid and T cell potential. (a and b) Flow cytometric analysis of cells harvested 10 d after adding 2,000 pre-pro–B cells (a) or early pro–B cells (b) in media containing SCF, Flt3L, and IL-7 to S17 stromal cell monolayers. (c) Yields of $CD19^+B220^+$ cells from cultures started with pre-pro–B or early pro–B cells as indicated below the graph. (d) Flow cytometric analysis of non–B cells in the $CD19^{lo}B220^{lo}$ gates in a. (e) Flow cytometric analysis of cells obtained 15 d after adding 2,000 pre-pro–B cells in media containing IL-6, -7, and -15 and Flt3L to OP9-DL1 stromal cell monolayers. All $Thy1.2^+CD49b^+$ cells expressed CD25 (not depicted). (f) Yields of cells obtained after plating pre-pro–B cells onto the indicated stromal cells. All data are representative of three independent experiments.

but the amount obtained was generally lower. In addition, PCR amplification of *Justy* cDNA gave rise to a prominent and unique 527-bp product that contained an 81-bp sequence inserted between exons 24 and 25. BLAT analysis (UCSC Genome Browser) showed that the insertion was derived from the intron between *Gon4l* exons 24 and 25. Gon4l mRNA containing the insertion was otherwise unaffected based on sequence analysis of PCR products anchored to the insertion.

The data described in the previous paragraph posited that intron 24 of *Gon4l* in *Justy* mice contains a mutation that causes the 81-bp element to be recognized as an exon. Sequence analysis of the *Justy* genome identified a T-to-A substitution immediately downstream of the 81-nt sequence that increases homology between the adjoining region and the consensus donor pre-mRNA splice site (Fig. 5 d). The structure of the 527-bp *Justy*-specific PCR product confirmed that this region is used as a donor splice site, resulting in fusion of the 81-nt sequence to exon 25. The structure of the 527-bp product also showed that a cryptic acceptor splice site in intron 24 mediates fusion of the 81-nt sequence to exon 24. Notably, inclusion of the 81-nt sequence into Gon4l mRNA places two premature termination codons into the open reading frame. However, the encoded protein was not detected when *Justy* cell lysates were immunoblotted with antibodies capable of recognizing it (unpublished data). This result suggests that inclusion of the 81-nt sequence, and thus the premature termination codons, activates the nonsense-mediated decay RNA surveillance pathway (Chang et al., 2007), preventing translation of the encoded protein.

Aberrant splicing of Gon4l RNA results in decreased expression of protein

It was not feasible to assess how the mutation affects Gon4l protein expression in the few B-lineage cells present in *Justy* mice. However, Northern blot analysis showed that Gon4l RNA was abundant in wild-type and *Justy* thymocytes (unpublished data). Immunoblotting of thymocyte lysates with antibodies specific for the C terminus of Gon4l showed that wild-type cells express this protein and that the level of Gon4l in *Justy* cells was greatly reduced (Fig. 5 e). To correlate this effect with altered Gon4l RNA splicing, Q RT-PCR analysis of thymocyte RNA was performed using primer pairs specific for either aberrantly spliced Gon4l RNA (i.e., containing the 81-nt insertion) or for wild-type Gon4l RNA (Fig. 5 f). Aberrantly

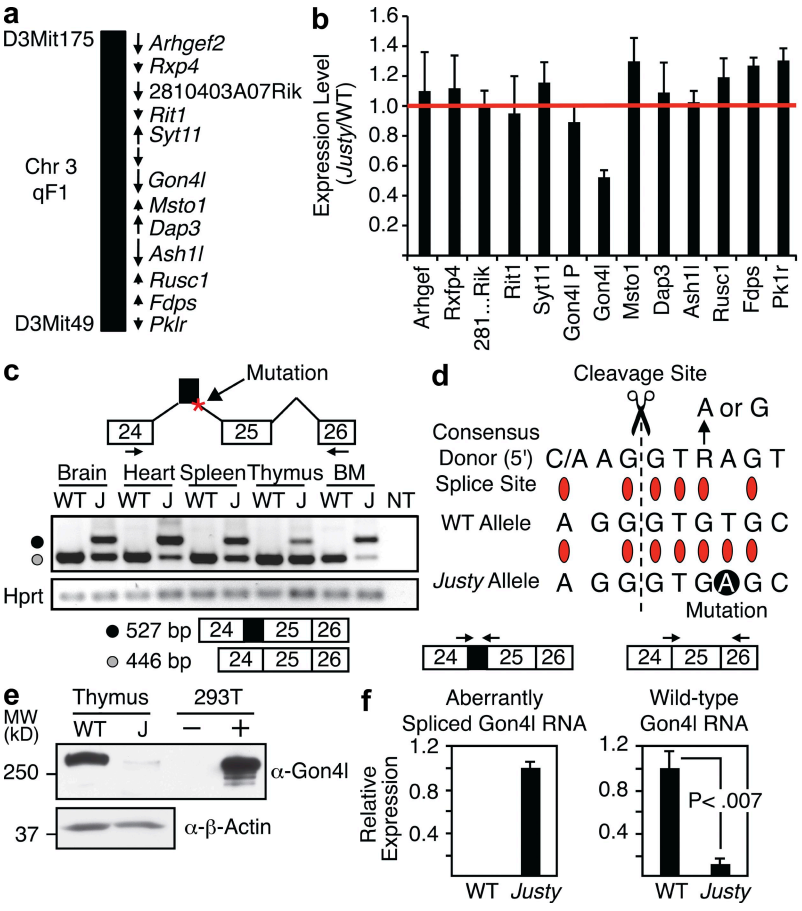

Figure 5. The *Justy* mutation disrupts synthesis of RNA and protein from the *Gon4l* gene. (a) Schematic showing the region of mouse chromosome 3 containing the *Justy* mutation. (b) Q RT-PCR analysis of gene expression in lineage-negative bone marrow cells. Three independent sets of wild-type and *Justy* cells were analyzed and values for each RNA were normalized to that for Hprt. Ratios between *Justy* and wild-type values (*Justy*/WT) were calculated for all RNAs. Shown are the ratio means and standard deviations from the three sets. (c) Schematic (top) of a portion of the *Gon4l* gene and the primers used for RT-PCR. The red asterisk denotes the *Justy* mutation. The black box represents the 81-bp insertion found in the 527-bp *Justy*-specific PCR product. Agarose gel (center) shows products from PCR amplification of cDNA from the indicated organs. BM, bone marrow. Structures of the Gon4l products seen are diagrammed (bottom). Hprt cDNA amplification indicated that all samples contained similar amounts of total cDNA. (d) Schematic shows that the *Justy* mutation (labeled) increases homology to the consensus donor splice site sequence. The same region from wild-type *Gon4l* is shown. Red ovals denote matches to the consensus splice site sequence. (e) Immunoblot of thymocyte lysates using Gon4l antibodies. Immunoblot for β-actin confirmed equal protein loading. Lysates from 293T cells transfected with a Gon4l expression plasmid (+) or empty vector (−) were used as controls. (f) Q RT-PCR analysis of aberrantly spliced and wild-type forms of Gon4l RNA in thymocytes. Diagrams at the top show the location of the PCR primers used relative to the Gon4l cDNA that was amplified. In the left graph, the wild-type value is relative to the *Justy* value, which was set at 1. In the right graph, the *Justy* value is relative to the wild-type value, which was set at 1. Error bars indicate standard error of the mean. All data are representative of three independent experiments.

spliced RNA was detected in *Justy* cells but not in wild type. Wild-type Gon4l RNA was observed in both wild-type and *Justy* thymocytes but the level in *Justy* cells was ∼10-fold lower. These data demonstrate that disruption of Gon4l RNA splicing as a result of the *Justy* mutation greatly reduces expression of wild-type Gon4l mRNA and thus protein.

Wild-type Gon4l RNA levels are greatly decreased in *Justy* B cell progenitors

Gon4l expression in B cell progenitors was assessed. Q RT-PCR analysis showed that Gon4l RNA is present at all stages of B lymphopoiesis and at elevated levels in later stages (Fig. 6 a). Immunoblot analysis of lysates prepared from wild-type pro–B cells grown in culture demonstrated that Gon4l was present (Fig. 6 b), which is consistent with the *Justy* phenotype. Gon4l was also detected in lysates from the mouse B cell line M12 (Fig. 6 b) or those from other mouse B cell lines (not depicted). Q RT-PCR analysis was performed to determine the levels of wild-type and aberrantly spliced Gon4l RNA in sort-purified pre-pro–B and early pro–B cells (Fig. 6 c). Similar to thymocytes, aberrantly spliced Gon4l RNA was detected only in *Justy* B cell progenitors. Wild-type Gon4l RNA was detected in both wild-type and *Justy* cells but the levels in *Justy* cells were greatly and significantly reduced. These data show that the *Justy* mutation dramatically reduces expression of wild-type Gon4l mRNA in B cell progenitors, an effect which was demonstrated to decrease Gon4l protein expression.

Gon4l encodes a protein with homology to transcriptional corepressors

As described for its orthologues (Liu et al., 2007; Ohtomo et al., 2007), mouse Gon4l contains regions with homology to transcriptional regulators (Fig. 6 d). A portion of Gon4l is 78% similar to human YY1AP (YY1-associated protein), so named because it interacts with the transcription factor YY1 (Wang et al., 2004). Two regions near the C terminus of Gon4l bear strong homology (E-values of 2.2 and 3.4 × 10^{-12}; from the SMART database) to the consensus paired amphipathic helix (PAH) repeat sequence, which forms a four-helix bundle (Brubaker et al., 2000). The mammalian transcriptional corepressors Sin3a and Sin3b each contain four PAH repeats, which mediate interactions with chromatin-modifying factors or DNA-binding proteins (Grzenda et al., 2009). NMR analysis (protein data bank accession code 1UG2) has shown that the C terminus of Gon4l forms a helix-loop-helix structure called a SANT domain (SWI3, ADA2, N-CoR, and TFIIIB; Boyer et al., 2004). Proteins containing this domain include the corepressor proteins SMRT and N-CoR. Lastly, the zebrafish and *C. elegans* Gon4l proteins can localize to the nucleus (Friedman et al., 2000; Liu et al., 2007). These features implicate Gon4l in pathways that mediate transcriptional regulation.

Regulation of gene expression is altered in *Justy* B cell progenitors

Q RT-PCR analysis was performed to assess how the *Justy* mutation affects gene expression in B cell progenitors. The development of pro–B cells requires the transcription factors E2A, EBF, and Pax5. *Justy* pre-pro–B and early pro–B cells expressed normal levels of RNA encoding these factors, except that the level of Pax5 RNA in *Justy* early pro–B cells was consistently but modestly elevated (Fig. 6 e). Consistent with these data, *Justy* cells expressed normal or slightly decreased levels of RNA encoding other B-lineage factors (Fig. S4).

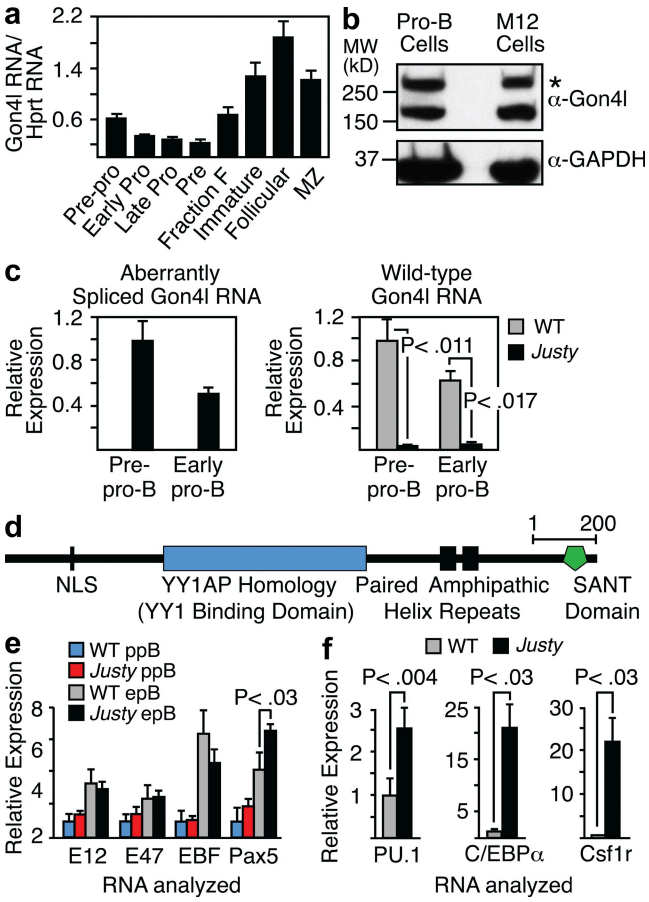

Figure 6. Decreased expression of Gon4l impairs gene repression in B cell progenitors. (a) Q RT-PCR analysis of Gon4l RNA in B cell fractions. PCR primers used targeted exon 33 and the 3′ UTR of Gon4l RNA. Values shown are normalized to Hprt values. (b) Immunoblot of wild-type pro–B cell lysate probed with Gon4l antibodies. Asterisk denotes full-length Gon4l. Generation of pro–B cells is described in Materials and methods. Lysate from the mouse B cell line M12 was included as a control. Probing for GAPDH confirmed equal protein loading. (c) Q RT-PCR analysis of aberrantly spliced and wild-type forms of Gon4l RNA in B cell progenitors. PCR primer pairs shown in Fig. 5 f were used for amplification. For the left graph, each value is relative to the *Justy* pre-pro–B cell value, which was set at 1. For the right graph, each value is relative to the wild-type pre-pro–B cell value, which was set at 1. (d) Schematic of the Gon4l protein. Structural motifs noted are described in the text. (e) Q RT-PCR analysis of RNA encoding the indicated proteins in B cell progenitors. For all RNAs, values are plotted relative to the wild-type pre-pro–B cell value, which was set at 1. (f) Q RT-PCR analysis of the indicated RNAs in early pro–B cells. Each *Justy* value is relative to the wild-type value, which was set at 1. All data are representative of three independent experiments. Error bars indicate standard error of the mean.

These findings suggest that decreased expression of E2A, EBF, or Pax5 is not responsible for the phenotype.

Progression of B lymphopoiesis has been correlated with decreased expression of RNA encoding PU.1 or C/EBPα (Rumfelt et al., 2006). Either of these transcription factors inhibits B lymphopoiesis when expressed at inappropriately high levels (DeKoter and Singh, 2000; Heavey et al., 2003; Xie et al., 2004; Hsu et al., 2006). As reported previously (Rumfelt et al., 2006), Q RT-PCR analysis of wild-type cells suggested that expression of PU.1 and C/EBPα RNA is down-regulated during the pre-pro–B to early pro–B cell transition (by factors of ∼4 and 46, respectively; unpublished data). In *Justy* pre-pro–B cells, the level of PU.1 RNA was slightly increased (∼1.4-fold), whereas that of C/EBPα RNA was significantly elevated (∼3.5-fold; $P < 0.025$) relative to that detected in wild-type cells. In *Justy* early pro–B cells, the levels of PU.1 and C/EBPα RNA were both significantly higher than those in wild-type cells, with the latter being increased by a factor of ∼20 (Fig. 6 f). Furthermore, comparison of Q RT-PCR data from *Justy* pre-pro–B and early pro–B cells suggested that mechanisms that down-regulate PU.1 and C/EBPα RNA expression are impaired. Consistent with these abnormalities, RNA encoded by the PU.1 and C/EBPα target gene *Csf1r* was expressed at elevated levels in *Justy* early pro–B cells relative to wild type (Fig. 6 f). These results suggest that loss of Gon4l expression impairs pathways that inhibit expression of PU.1 and C/EBPα RNA in developing B cells.

Gon4l orthologues are present in the genomes of plants, invertebrates, and vertebrates (Kuryshev et al., 2006) and is highly conserved among the latter. Similar to our study, forward-genetic studies involving *C. elegans* and zebrafish have demonstrated that *Gon4l* is important for specific developmental pathways (Friedman et al., 2000; Liu et al., 2007). Homozygosity for loss-of-function *Gon4l* alleles in zebrafish cause embryologic abnormalities and death soon after conception (Liu et al., 2007). Furthermore, such mutations disrupt erythropoiesis and the expression of key erythroid genes (Liu et al., 2007), suggesting that *Gon4l* is required for hematopoietic development. In addition, loss of Gon4l expression in zebrafish appears to affect pathways that control cell cycle progression (Liu et al., 2007; Lim et al., 2009). Ours is the first study to demonstrate that *Gon4l* has an important role in mammalian hematopoiesis.

Gon4l RNA is expressed throughout zebrafish embryos (Liu et al., 2007) and is broadly expressed in mammals (Kuryshev et al., 2006; Ohtomo et al., 2007, 2008). Our data show that Gon4l RNA and protein are expressed in B-lineage cells and thymocytes, indicating that Gon4l is not a B-lineage–specific factor. Why the *Justy* mutation seems to affect only B lymphopoiesis is not clear. Perhaps the role of Gon4l varies between cell lineages and tissues, which suggests that additional but subtler phenotypes might exist. Another factor that may contribute to the specificity of the phenotype is variation between tissues in the extent of aberrant Gon4l pre-mRNA splicing and, thus, the decrease in wild-type Gon4l RNA and protein expression. Indeed, Q RT-PCR analysis of wild-type Gon4l RNA levels in tissues from wild-type and *Justy* mice showed that such variation occurs (Fig. S5). These data suggest the *Justy* mutation has created a conditional loss-of-function *Gon4l* allele rather than a completely nonfunctional one. Further analysis of *Justy* mice and the Gon4l protein will address these issues and will likely yield novel insights regarding mechanisms that regulate B lymphopoiesis.

MATERIALS AND METHODS

Mice. Mutagenesis, breeding, and positional cloning have been previously described (Hrabé de Angelis et al., 2000; Augustin et al., 2005). Mice were used in compliance with the United States Department of Health and Human Services Guide for Use of Laboratory Animals, as documented in writing and approved by the University of Iowa Animal Care and Use Committee.

Bone marrow transplantation. Recipients were given 1,100 rads of irradiation. 1 h later, 10^7 red blood cell–depleted bone marrow cells were injected into the retro-orbital plexus. Recipients were given drinking water containing antibiotic (Baytril) for 3 wk afterward and analyzed 5 wk later.

Flow cytometric analysis and cell sorting. Cells were suspended in PBS containing 3% FBS and preincubated with anti-CD16/32. Cells were incubated with fluorochrome- or biotin-conjugated antibodies for 30 min on ice and washed. When necessary, cells were resuspended in buffer containing streptavidin- or avidin-conjugated fluorophore, incubated for 30 min on ice, and washed. Flow cytometric analysis was performed using an LSR II or a FACSDiva (BD) and data were analyzed using FlowJo (Tree Star, Inc.). A FACSDiva was used to sort purify cells. To isolate cells at the pre–B cell stage onward, splenocytes or bone marrow cells were stained and sorted. To isolate pre-pro–B and early pro–B cells from bone marrow, a negative selection step was included. Cells were incubated with rat anti–mouse Ter-119, CD5, Ly6C, and IgM, washed, and then incubated with magnetic beads coated with sheep anti–rat antibodies (Invitrogen). Beads and bound cells were removed and remaining cells were stained and sorted. Intracellular staining for phospho-Stat5 was performed using a PE-labeled mouse anti–phospho-Stat5 antibody according to the manufacturer's (BD) instructions.

Antibodies. The following fluorochrome-conjugated antibodies were purchased from the listed sources or generated in the Waldschmidt Laboratory: Alexa Fluor 700-B220 (RA3-6B2), APC-c-Kit (2B8), and APC-CD24/HSA (M1/69; BioLegend); Sca-1 (D7; Pacific Blue); APC conjugates B220 (RA3-6B2) and CD3ε (145-2C11), FITC conjugates CD11c (N418) and CD49b (DX5), PE conjugates BP-1 (6C3) and CD25 (PC61.5), and PE-Cy7 conjugates CD11c (N418) and CD19 (1D3; eBioscience); APC-Thy-1.2 (53–2.1), APC-Cy7-B220 (RA3-6B2), PE-Gr-1 (RB6-8C5), and PerCP-B220 (RA3-6B2) and Biotin conjugates CD11b/Mac-1 (M1/70), Gr-1 (RB6-8C5), CD43 (S7), CD49b (DX5), CD11c (N418), Ter-119, CD3ε (145-2C11), and CD19 (APC-H7; BD); Avidin-Texas Red and Streptavidin Per-CP (BD); Streptavidin Qdot 605 (Invitrogen); FITC-Ly6d (RGRSL 114.8.1; Sigma-Aldrich); Cy5-, FITC-, PE- and PE-Cy7-B220 (RA3-6B2) and FITC-CD3ε (145-2C11), Texas Red-CD45.1 (A20), FITC-CD45.2 (104), PE-CD4 (GK1.5), Cy5-CD8α (53–6.7), FITC-CD21 (7E9), PE-CD23 (B3B4), Cy5-IgM (B76), and FITC-Ly6C (Waldschmidt Laboratory).

Stromal cell co-cultures. To test for B and myeloid potential, 2,000 sorted cells were added to 24-well plates containing S17 stromal cells (Collins and Dorshkind, 1987) in media containing SCF, Flt3L, and IL-7 at 10 ng/ml each. To test for T/NK cell potential, 2,000 sorted cells were added to wells containing OP9-DL1 stromal cells (Schmitt and Zúñiga-Pflücker, 2002) in media containing 1 ng/ml IL-6, 10 ng/ml IL-7, 10 ng/ml Flt3L, and 25 ng/ml IL-15. 10 or 15 d later, cells were harvested and analyzed by flow cytometry. S17 cultures were stained for Ly6C, Gr-1, CD11b, B220, and CD19; OP9-DL1 cultures were stained for Thy-1.2, CD25, CD49b (DX5), B220, and CD19.

Pro–B cells were generated by adding Lin^- cells to layers of OP9 stromal cells in media containing SCF, Flt3L, and IL-7 at 10 ng/ml each. Lin^- cells were isolated by negative selection (as described in the Flow cytometric analysis and cell sorting section) except that antibodies for CD19 and B220 were included. Cultures were started in 24-well plates and expanded over a 3-wk period. > 90% of the cells obtained were $B220^+CD19^+$.

RT-PCR analysis. RNA was isolated using TRIzol (Invitrogen) and reverse transcribed using SuperScript III (Invitrogen). Conventional PCR was performed using AmpliTaq Gold (Applied Biosystems) and a MyCycler (Bio-Rad Laboratories). Quantitative real-time PCR was performed using POWER SYBR Green Master Mix and the PRISM 7700 Detection system (Applied Biosystems) to obtain cycle threshold (Ct) values for target and internal reference (Hprt) cDNAs. Target cDNA levels were normalized to Hprt cDNA levels using the Eq. $2^{-[\Delta Ct]}$, where ΔCt is defined as $Ct_{target} - Ct_{Hprt}$.

Antibody production and immunoblot analysis. cDNA encoding Gon4l aa 938–1364 or 1746–2260 was cloned into the plasmid pGEX-5-1 (GE Healthcare). GST-Gon4l fusion proteins were expressed in bacteria and purified using glutathione-agarose beads. Fusion proteins were cleaved with Factor Xa (GE Healthcare) and resolved by SDS-PAGE. Rabbits were immunized three to five times with gel slices containing Gon4l protein. Immunoglobulins from pooled bleeds were purified by protein A–Sepharose and affinity selection and used for immunoblot analysis. Protein lysates were prepared by resuspending cells in RIPA buffer containing protease inhibitors (Roche). Immunoblot analysis used standard protocols.

Online supplemental material. Fig. S1 shows flow cytometric analysis and quantification of hematopoietic and myeloid progenitors in bone marrow. Fig. S2 shows flow cytometric analysis and quantification of CLPs in bone marrow. Fig. S3 shows flow cytometric analysis of IL-7Rα expression and phospho-Stat5 levels in B cell progenitors. Fig. S4 shows Q RT-PCR analysis of B lineage gene expression in B cell progenitors. Fig. S5 shows the ratio of normal Gon4l RNA detected in tissues from Justy or wild-type mice as determined by Q RT-PCR analysis. Online supplemental material is available at http://www.jem.org/cgi/content/full/jem.20100147/DC1.

We thank Lorraine Tygrett for help with bone marrow transplants and antibody preparations, and the University of Iowa Flow Cytometry Facility and Teresa Duling for help with flow cytometry. We thank the University of Iowa DNA Facility for help with real-time PCR analysis.

This work was supported by funds from the Internal Medicine Department, University of Iowa, and the National Institutes of Health/National Institute of Allergies and Infectious Disease (R01AI067489, awarded to J.D. Colgan).

The authors have no conflicting financial interests.

Submitted: 22 January 2010
Accepted: 29 April 2010

REFERENCES

Akashi, K., D. Traver, T. Miyamoto, and I.L. Weissman. 2000. A clonogenic common myeloid progenitor that gives rise to all myeloid lineages. *Nature*. 404:193–197. doi:10.1038/35004599

Augustin, M., R. Sedlmeier, T. Peters, U. Huffstadt, E. Kochmann, D. Simon, M. Schöniger, S. Garke-Mayerthaler, J. Laufs, M. Mayhaus, et al. 2005. Efficient and fast targeted production of murine models based on ENU mutagenesis. *Mamm. Genome*. 16:405–413. doi:10.1007/s00335-004-3028-2

Balciunaite, G., R. Ceredig, S. Massa, and A.G. Rolink. 2005. A B220+ CD117+ CD19- hematopoietic progenitor with potent lymphoid and myeloid developmental potential. *Eur. J. Immunol.* 35:2019–2030. doi:10.1002/eji.200526318

Beutler, B., X. Du, and Y. Xia. 2007. Precis on forward genetics in mice. *Nat. Immunol.* 8:659–664. doi:10.1038/ni0707-659

Boyer, L.A., R.R. Latek, and C.L. Peterson. 2004. The SANT domain: a unique histone-tail-binding module? *Nat. Rev. Mol. Cell Biol.* 5:158–163. doi:10.1038/nrm1314

Brown, G., P.J. Hughes, R.H. Michell, A.G. Rolink, and R. Ceredig. 2007. The sequential determination model of hematopoiesis. *Trends Immunol.* 28:442–448. doi:10.1016/j.it.2007.07.007

Brubaker, K., S.M. Cowley, K. Huang, L. Loo, G.S. Yochum, D.E. Ayer, R.N. Eisenman, and I. Radhakrishnan. 2000. Solution structure of the interacting domains of the Mad-Sin3 complex: implications for recruitment of a chromatin-modifying complex. *Cell*. 103:655–665. doi:10.1016/S0092-8674(00)00168-9

Chang, Y.F., J.S. Imam, and M.F. Wilkinson. 2007. The nonsense-mediated decay RNA surveillance pathway. *Annu. Rev. Biochem.* 76:51–74. doi:10.1146/annurev.biochem.76.050106.093909

Collins, L.S., and K. Dorshkind. 1987. A stromal cell line from myeloid long-term bone marrow cultures can support myelopoiesis and B lymphopoiesis. *J. Immunol.* 138:1082–1087.

Cook, M.C., C.G. Vinuesa, and C.C. Goodnow. 2006. ENU-mutagenesis: insight into immune function and pathology. *Curr. Opin. Immunol.* 18:627–633. doi:10.1016/j.coi.2006.07.011

DeKoter, R.P., and H. Singh. 2000. Regulation of B lymphocyte and macrophage development by graded expression of PU.1. *Science*. 288:1439–1441. doi:10.1126/science.288.5470.1439

Eberhard, D., G. Jiménez, B. Heavey, and M. Busslinger. 2000. Transcriptional repression by Pax5 (BSAP) through interaction with corepressors of the Groucho family. *EMBO J.* 19:2292–2303. doi:10.1093/emboj/19.10.2292

Friedman, L., S. Santa Anna-Arriola, J. Hodgkin, and J. Kimble. 2000. gon-4, a cell lineage regulator required for gonadogenesis in Caenorhabditis elegans. *Dev. Biol.* 228:350–362. doi:10.1006/dbio.2000.9944

Fuxa, M., J. Skok, A. Souabni, G. Salvagiotto, E. Roldan, and M. Busslinger. 2004. Pax5 induces V-to-DJ rearrangements and locus contraction of the immunoglobulin heavy-chain gene. *Genes Dev.* 18:411–422. doi:10.1101/gad.291504

Gao, H., K. Lukin, J. Ramírez, S. Fields, D. Lopez, and J. Hagman. 2009. Opposing effects of SWI/SNF and Mi-2/NuRD chromatin remodeling complexes on epigenetic reprogramming by EBF and Pax5. *Proc. Natl. Acad. Sci. USA*. 106:11258–11263. doi:10.1073/pnas.0809485106

Grzenda, A., G. Lomberk, J.S. Zhang, and R. Urrutia. 2009. Sin3: master scaffold and transcriptional corepressor. *Biochim. Biophys. Acta*. 1789:443–450.

Hardy, R.R., P.W. Kincade, and K. Dorshkind. 2007. The protean nature of cells in the B lymphocyte lineage. *Immunity*. 26:703–714. doi:10.1016/j.immuni.2007.05.013

Heavey, B., C. Charalambous, C. Cobaleda, and M. Busslinger. 2003. Myeloid lineage switch of Pax5 mutant but not wild-type B cell progenitors by C/EBPalpha and GATA factors. *EMBO J.* 22:3887–3897. doi:10.1093/emboj/cdg380

Hrabé de Angelis, M.H., H. Flaswinkel, H. Fuchs, B. Rathkolb, D. Soewarto, S. Marschall, S. Heffner, W. Pargent, K. Wuensch, M. Jung, et al. 2000. Genome-wide, large-scale production of mutant mice by ENU mutagenesis. *Nat. Genet.* 25:444–447. doi:10.1038/78146

Hsu, C.L., A.G. King-Fleischman, A.Y. Lai, Y. Matsumoto, I.L. Weissman, and M. Kondo. 2006. Antagonistic effect of CCAAT enhancer-binding protein-alpha and Pax5 in myeloid or lymphoid lineage choice in common lymphoid progenitors. *Proc. Natl. Acad. Sci. USA*. 103:672–677. doi:10.1073/pnas.0510304103

Inlay, M.A., D. Bhattacharya, D. Sahoo, T. Serwold, J. Seita, H. Karsunky, S.K. Plevritis, D.L. Dill, and I.L. Weissman. 2009. Ly6d marks the earliest stage of B-cell specification and identifies the branchpoint between B-cell and T-cell development. *Genes Dev.* 23:2376–2381. doi:10.1101/gad.1836009

Koipally, J., and K. Georgopoulos. 2002. A molecular dissection of the repression circuitry of Ikaros. *J. Biol. Chem.* 277:27697–27705. doi:10.1074/jbc.M201694200

Kuryshev, V.Y., E. Vorobyov, D. Zink, J. Schmitz, T.S. Rozhdestvensky, E. Münstermann, U. Ernst, R. Wellenreuther, P. Moosmayer, S. Bechtel, et al. 2006. An anthropoid-specific segmental duplication on human chromosome 1q22. *Genomics*. 88:143–151. doi:10.1016/j.ygeno.2006.02.002

Laiosa, C.V., M. Stadtfeld, and T. Graf. 2006. Determinants of lymphoid-myeloid lineage diversification. *Annu. Rev. Immunol.* 24:705–738. doi:10.1146/annurev.immunol.24.021605.090742

Lim, C.H., S.W. Chong, and Y.J. Jiang. 2009. Udu deficiency activates DNA damage checkpoint. *Mol. Biol. Cell.* 20:4183–4193. doi:10.1091/mbc.E09-02-0109

Liu, Y., L. Du, M. Osato, E.H. Teo, F. Qian, H. Jin, F. Zhen, J. Xu, L. Guo, H. Huang, et al. 2007. The zebrafish udu gene encodes a novel nuclear factor and is essential for primitive erythroid cell development. *Blood.* 110:99–106. doi:10.1182/blood-2006-11-059204

Mansson, R., S. Zandi, E. Welinder, P. Tsapogas, N. Sakaguchi, D. Bryder, and M. Sigvardsson. 2010. Single-cell analysis of the common lymphoid progenitor compartment reveals functional and molecular heterogeneity. *Blood.* 115:2601–2609. doi:10.1182/blood-2009-08-236398

Ng, S.Y., T. Yoshida, and K. Georgopoulos. 2007. Ikaros and chromatin regulation in early hematopoiesis. *Curr. Opin. Immunol.* 19:116–122. doi:10.1016/j.coi.2007.02.014

Nutt, S.L., and B.L. Kee. 2007. The transcriptional regulation of B cell lineage commitment. *Immunity.* 26:715–725. doi:10.1016/j.immuni.2007.05.010

O'Neil, J., and A.T. Look. 2007. Mechanisms of transcription factor deregulation in lymphoid cell transformation. *Oncogene.* 26:6838–6849. doi:10.1038/sj.onc.1210766

Ohtomo, T., T. Horii, M. Nomizu, T. Suga, and J. Yamada. 2007. Molecular cloning of a structural homolog of YY1AP, a coactivator of the multifunctional transcription factor YY1. *Amino Acids.* 33:645–652. doi:10.1007/s00726-006-0482-z

Ohtomo, T., T. Horii, M. Nomizu, T. Suga, and J. Yamada. 2008. Cloning and expression analysis of YY1AP-related protein in the rat brain. *Amino Acids.* 34:155–161. doi:10.1007/s00726-006-0483-y

Reynaud, D., I.A. Demarco, K.L. Reddy, H. Schjerven, E. Bertolino, Z. Chen, S.T. Smale, S. Winandy, and H. Singh. 2008. Regulation of B cell fate commitment and immunoglobulin heavy-chain gene rearrangements by Ikaros. *Nat. Immunol.* 9:927–936. doi:10.1038/ni.1626

Rosenbauer, F., and D.G. Tenen. 2007. Transcription factors in myeloid development: balancing differentiation with transformation. *Nat. Rev. Immunol.* 7:105–117. doi:10.1038/nri2024

Rumfelt, L.L., Y. Zhou, B.M. Rowley, S.A. Shinton, and R.R. Hardy. 2006. Lineage specification and plasticity in $CD19^{-}$ early B cell precursors. *J. Exp. Med.* 203:675–687. doi:10.1084/jem.20052444

Schmitt, T.M., and J.C. Zúñiga-Pflücker. 2002. Induction of T cell development from hematopoietic progenitor cells by delta-like-1 in vitro. *Immunity.* 17:749–756. doi:10.1016/S1074-7613(02)00474-0

Wang, C.Y., Y.J. Liang, Y.S. Lin, H.M. Shih, Y.S. Jou, and W.C. Yu. 2004. YY1AP, a novel co-activator of YY1. *J. Biol. Chem.* 279:17750–17755. doi:10.1074/jbc.M310532200

Welner, R.S., R. Pelayo, and P.W. Kincade. 2008. Evolving views on the genealogy of B cells. *Nat. Rev. Immunol.* 8:95–106. doi:10.1038/nri2234

Xie, H., M. Ye, R. Feng, and T. Graf. 2004. Stepwise reprogramming of B cells into macrophages. *Cell.* 117:663–676. doi:10.1016/S0092-8674(04)00419-2